Studies on the Steady and Dynamic Rheological Properties of Poly(dimethyl-siloxane) Filled with Calcium Carbonate Based On Superposition of Its Relative Functions

Xiaoming Xu,[1] Xiaole Tao,[2,3] Chuanhua Gao,[1] Qiang Zheng[1,2]

[1]*Department of Polymer Science and Engineering, Zhejiang University, Hangzhou 310027, People's Republic of China*
[2]*Department of Chemistry, Zhejiang University, Hangzhou 310027, People's Republic of China*
[3]*R&D Center, Hangzhou Zhijiang Silicone Co., Ltd., Hangzhou 311203, People's Republic of China*

Received 11 April 2007; accepted 1 September 2007
DOI 10.1002/app.27256
Published online 16 October 2007 in Wiley InterScience (www.interscience.wiley.com).

ABSTRACT: The steady and dynamic rheological properties of hydroxyl-terminated polydimethylsiloxane filled with calcium carbonate were investigated by varying the filler volume fraction (Φ) from 0 to 18.2 vol %. The results reveal that there exists a ''percolation threshold'' (Φ_c = 3.6%) for the suspensions, below which both the ''Cox-Merz'' and modified ''Cox-Merz'' rule are competent over the whole shear regions. However, these two rules breakdown and a characteristic plateau appears in low frequency regions for suspensions with $\Phi > \Phi_c$. The reasons for this can be ascribed to the contributions of nonhydrodynamic forces and formation of percolated filler network structure with increasing Φ. Moreover, using a concentration-dependent parameter, $B(\Phi)$, superposition curves of dynamic complex modulus ($|G^*|$) and shear stress (τ) for all suspensions were obtained through shifting $|G^*|$ curves along the ordinate and τ functions along the abscissa using different $B(\Phi)$ as shifting factor. Unfortunately, the reasonable superposition range is restricted in the high ω or $\dot{\gamma}$ regions. © 2007 Wiley Periodicals, Inc. J Appl Polym Sci 107: 1590–1597, 2008

Key words: polydimethylsiloxane; rheological properties; Cox-Merz rule; filler network; percolation threshold

INTRODUCTION

In general, polymers are endowed with a great quantity of advantages in case of incorporation of inorganic filler particles into them, such as increased strength and enhanced electrical conductivity over the virgin polymer systems. Recently, these aspects have attracted researchers' attention because of their academic interests and applied significance in industrial situations such as paints, foods, cosmetics, sealants, and automobile tire tread compound.[1–3] Silicone sealants, which are usually composed of hydroxyl-terminated polydimethylsiloxane (PDMS) and fillers, are widely used in construction and decoration fields. Compared with fumed silica (SiO_2), calcium carbonate ($CaCO_3$) has been extensively employed in the sealant industry because of its several remarkable benefits such as abundant raw material resource, low price, and stable properties.[4–6]

Correspondence to: Q. Zheng (zhengqiang@zju.edu.cn).
Contract grant sponsor: National Basic Research Program of China; contract grant number: 2005CB623800.
Contract grant sponsor: Key Program of the National Natural Science Foundation of China; contract grant number: 50633030.

Journal of Applied Polymer Science, Vol. 107, 1590–1597 (2008)

Understanding the interaction mechanism between incorporated fillers and polymer matrix is believed to be a key to explore the source of reinforcement by filler. It has been accepted that measurement of the dynamic rheological properties of filled polymers is a well-established approach to probe the interaction between filler and polymer matrix.[7,8] In other words, studies on the rheological behavior of such systems could provide insight into the structural development of samples. However, to our knowledge, few works concerning the rheological properties of PDMS filled with $CaCO_3$ particles have been reported except our pervious work.[9,10]

The so-called ''*Cox-Merz*'' rule, involving the shear rate ($\dot{\gamma}$) dependence of steady shear viscosity ($\eta(\dot{\gamma})$) and frequency (ω) dependence of dynamic complex viscosity ($|\eta^*(\omega)|$) as given as

$$\eta(\dot{\gamma}) = \left|\eta^*(\omega)\right|_{\omega=\dot{\gamma}} \quad (1)$$

This has extensively been employed for transforming rheological data or for checking consistency of data collected through different experimental modes.[11] This rule gives an astonishing simple relationship that predicts $|\eta^*(\omega)|$ and $\eta(\dot{\gamma})$ are equivalent when ω is equal to $\dot{\gamma}$, and has been found to be of great significance in polymer rheological research and

applications. For example, it is difficult to measure $\eta(\dot{\gamma})$ at high $\dot{\gamma}$ regions for many polymeric systems because of sample fracture, secondary flows, and so forth. Accordingly, the ''Cox-Merz'' rule can be used to predict $\eta(\dot{\gamma})$ of a material from dynamic measurements.[12] This rule can also be used to predict $|\eta^*(\omega)|$ from $\eta(\dot{\gamma})$ in case of the dynamic operating mode is unavailable. Furthermore, the rule can also be used to investigate the microstructure of materials from degree to which they adhere to the rule.

It is well known that besides the viscosity, dynamic complex modulus ($|G^*(\omega)|$) and shear stress ($\tau(\dot{\gamma})$) functions of materials collected through different experimental modes are also of great importance for their industrial applications. Hence, we introduce a modified formulation of the ''Cox-Merz'' rule based on eq. (1) to investigate the $|G^*(\omega)|$ and $\tau(\dot{\gamma})$. Using the definition of steady shear viscosity, $\eta(\dot{\gamma}) = \tau(\dot{\gamma})/\dot{\gamma}$, and of dynamic complex viscosity, $|\eta^*(\omega)| = |G^*(\omega)|/\omega$, the $\tau(\dot{\gamma})$ can be defined in terms of the $|G^*(\omega)|$ as given by

$$\tau(\dot{\gamma}) = \left|G^*(\omega)\right|_{\omega=\dot{\gamma}} \quad (2)$$

Although several literatures related to the application of ''Cox-Merz'' rule in some particle filled polymer systems could be found,[13–17] few studies concerning this rule on PDMS/$CaCO_3$ system have been reported up-to-date. In particular, little information is available on the modified ''Cox-Merz'' rule dealing with ω dependence of $|G^*(\omega)|$ and $\dot{\gamma}$ dependence of $\tau(\dot{\gamma})$ for the PDMS/$CaCO_3$ suspensions. The aim of the present article is to investigate the interactions between $CaCO_3$ filler and PDMS matrix through steady and dynamic measurements by varying the particle volume fraction. Through a comparison between the steady and dynamic rheological properties of PDMS/$CaCO_3$ suspensions based on the ''Cox-Merz'' and modified ''Cox-Merz'' rule, we try to predict the steady shear functions in the high $\dot{\gamma}$ regions from dynamic tests without extensive alternation of sample structures.

EXPERIMENTAL

Materials and sample preparation

The hydroxyl-terminated PDMS and $CaCO_3$ filler were commercial products from GE Toshiba Silicones, Japan, and Henan Keli New Material, China, respectively, (Table I). The $CaCO_3$ fillers were incorporated into PDMS over the volume fraction range from 0 to 18.2 vol % by a planetary mixer (XSJ-2, Chengdu Keqiang Polymer Engineering, China) with a rotor speed of 50 rpm at room temperature. The mixing procedure was conducted as follows: (1) PDMS was added into the planetary mixer and softened for 10 min without filler; (2) $CaCO_3$ was added and mixed for 30 min, and then degassed under vacuum condition to eliminate the effect of air on the rheological behavior of final samples. Consequently, the suspensions were further mixed for 90 min to ensure a uniform dispersion of fillers. Finally, the suspensions were extruded in a plastic cylinder (310-mL) for storage and measurements.

TABLE I
Typical Properties of PDMS and $CaCO_3$

PDMS	M_w = 125,734; M_n = 62,993; PDI = 1.996; η = 50,000 cp at 25°C; specific gravity = 0.98 g/cm^3
$CaCO_3$	N_2 (BET) surf. area = 25 m^2/g; particle diameter = 50 nm; DOP adsorption = 24 g/100 g $CaCO_3$; specific gravity = 2.65 g/cm^3

Properties measurements

The steady shear and dynamic measurements were performed on a stress-controlled rheometer (AR-G2, TA Instruments, USA) equipped with 40 mm diameter parallel-plate fixture at gap of 1 mm. The steady and dynamic data were obtained from shear rate sweep of 0.01–1000 s^{-1} and frequency sweep of 0.01–600 rad/s, respectively. For a parallel-plate measuring geometry, the shear rate and shear stress experienced by the sample during tests vary with radial position. Hence, the steady-state data were corrected by using the stress correction transformation function of the rheometer. The stress magnitude (1 Pa) exerted in the dynamic experiments was within linear viscoelastic range, which was determined by performing stress sweep at 6.28 rad/s. All experiments were carried out at a constant temperature of 25°C.

Morphological observation

Transmission electron microscopy (TEM, JEM 1200EX, Electron, Japan) was used for observing the filler dispersion. Vulcanized samples were microtomed and sections of 100 nm were obtained for observation.

RESULTS AND DISCUSSION

Figure 1 presents the plots of steady and dynamic functions versus $\dot{\gamma}$ and ω for virgin PDMS measured at 25°C. It can be found that there exists a Newtonian region ($\dot{\gamma}$ or $\omega < 30$ s^{-1}) for both the two viscosity curves in which $\eta(\dot{\gamma})$ is equal to $|\eta^*(\omega)|$, indicating the polymer matrix used here obeys the ''Cox-Merz'' rule; whereas a shear thinning region appears for $|\eta^*(\omega)|$ when $\dot{\gamma}$ or ω is beyond 30 s^{-1}, which can be explained by considering the disentanglement of polymer chains in a shear field. Mean-

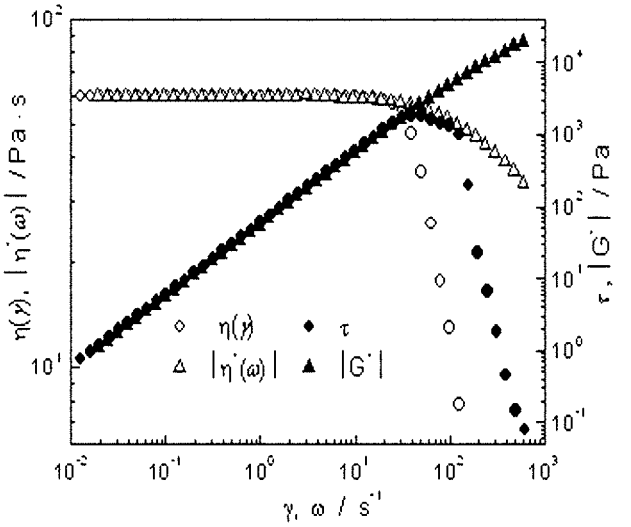

Figure 1 Steady shear (circular) and dynamic functions (triangle) versus shear rate ($\dot{\gamma}$) and frequency (ω) measured at 25°C for the virgin PDMS.

while, $\eta(\dot{\gamma})$ is noted to be apart from the onset of flow stabilities and the reason for this is attributed to the sample structure fracture upon high shear rates. In this situation, the ''Cox-Merz'' rule can be used to predict the steady properties in high $\dot{\gamma}$ regions from dynamic tests without extensive alternation of sample structures. Similar behavior was observed for the $\tau(\dot{\gamma})$ and $|G^*(\omega)|$ functions, indicating the validity of the modified ''Cox-Merz'' rule. Accordingly, it is expected that the virgin PDMS used here would obey the ''Cox-Merz'' and modified ''Cox-Merz'' rule over the whole $\dot{\gamma}$ or ω regions providing no sample structure fracture occurred.

Figure 2 gives the ω dependence of $|G^*|$ for PDMS/$CaCO_3$ suspensions with different filler volume fraction (Φ) measured at 25°C and 1 Pa. It can be found that $|G^*|$ increases with increasing Φ over the whole ω regions, which has been attributed to that the modulus layer resulting from polymer matrix surrounding filler particles becomes stronger due to the solidification of polymer chains onto particle surfaces.[9,10] Additionally, there exists a critical Φ (Φ_c = 3.6%) in low ω regions, referred to as ''percolation threshold,'' beyond which the suspensions display an ω-independent rheological behavior. This phenomenon can be observed more clearly from the dynamic storage modulus (G') versus ω curve as shown in the inset of Figure 2. The reasons for the transformation from liquid-like to solid-like behavior are extensively considered to be the formation of three-dimensional ordered structure such as framework, filler network, agglomerates, and so on.[9,10,18] Figure 3 gives the TEM images of vulcanized samples with different Φ (1.8%, 3.6%, 10%), in which the bright region represents PDMS phase while the dark region represents filler particles. It can be seen that when Φ increases up to Φ_c the particles intercontact with each other and form a filler network, indicating an agreement with the statements above.

On the other hand, it is interesting that all the curves, regardless of their filler volume fraction, are seem to be parallel in log–log scale in high ω regions (>5 rad/s), demonstrating that the $|G^*|$ value of each suspension divided by that of the polymer matrix is a function of Φ only as given as

$$\frac{|G^*(\omega,\Phi)|}{|G^*(\omega,\Phi=0)|}=f(\Phi) \tag{3}$$

Equation (3) illustrates that in the high ω regions (>5 rad/s), the viscoelastic behavior of suspensions is dominated by polymer matrix. As a result, the $CaCO_3$ particles' contribution to any modification of the relaxation time is negligible. Similar trends have also been observed in case of PDMS filled with glass beads.[19] Hence, to investigate the concentration-dependent changes in rheological properties, we introduce a parameter, B, which depends only on the Φ.

Figure 4 depicts the schematic plot of determination for parameter B_{dy} through polymer matrix and its corresponding suspension with Φ = 10%, where the subscript dy stands for dynamic shear conditions. It can be seen that in the high ω regions the distance between the two curves along $|G^*|$ axis is identical, and B_{dy} can be defined here as the quotient of $|G^*|$ value for the suspension and that of the polymer matrix conducted at the same ω as given as

$$B_{dy}=\frac{|G^*(\omega_1)|_{Susp}}{|G^*(\omega_1)|_P}=\frac{|G^*(\omega_2)|_{Susp}}{|G^*(\omega_2)|_P}=f(\Phi) \tag{4}$$

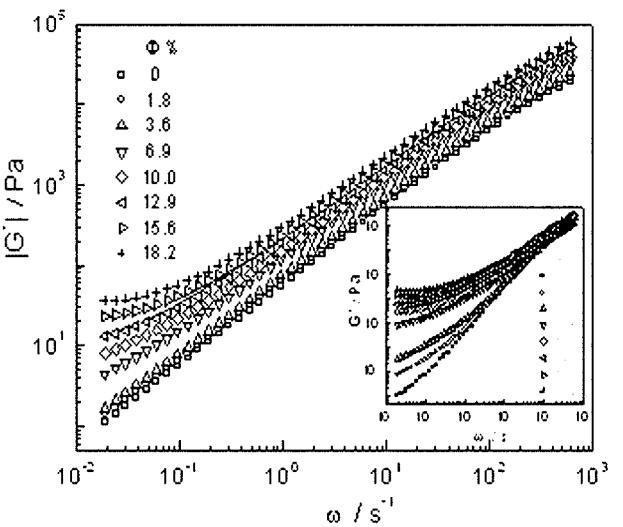

Figure 2 Frequency (ω) dependence of complex modulus ($|G^*|$) for PDMS/$CaCO_3$ suspensions with different filler volume fraction (Φ) at 25°C. The inset shows the ω dependence of dynamic storage modulus (G') for the same samples.

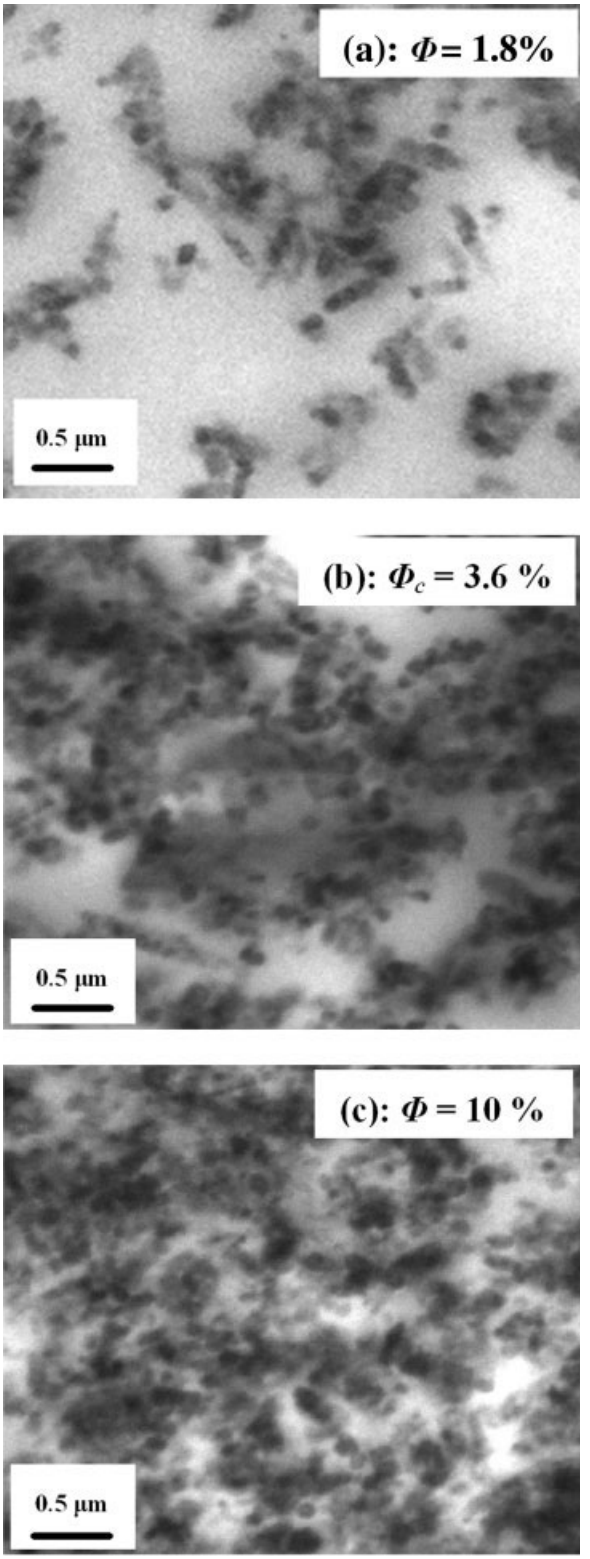

Figure 3 TEM (×30,000) images of vulcanized PDMS/$CaCO_3$ suspensions with different filler volume fraction (Φ): (a) 1.8%, (b) 3.6%, (c)10%.

where the subscript *P* and Susp stand for polymer matrix and suspensions, respectively. Equation (4) suggests that in high ω regions, a superposition

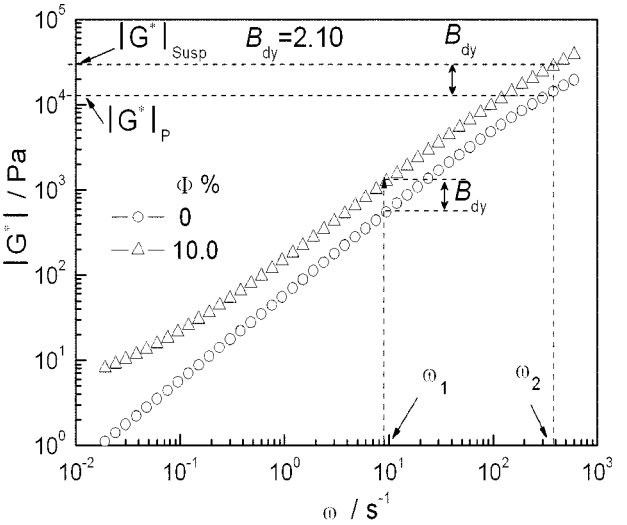

Figure 4 Experimental graphic determination of shifting factor (B_{dy}).

curve of $|G^*|$ versus ω for all suspensions could be portrayed by using B_{dy} as a shifting factor.

Figure 5 presents the superposition curve of $|G^*|$ versus ω for PDMS/$CaCO_3$ suspensions with different Φ through dividing the $|G^*|$ value of suspensions by their corresponding B_{dy}. It is obvious that the curves of suspension with $\Phi < \Phi_c$ could collapse on the virgin PDMS curve reasonably in the whole ω regions. For suspensions with $\Phi > \Phi_c$, the superposition still holds in the high ω regions; however, discrepancies appear with decreasing ω. The reason for this phenomenon can be ascribed to the formation of percolated filler network structure because of filler–filler and filler–polymer interactions. On the other hand, an apparent yielding phenomenon appearing in suspensions with $\Phi > \Phi_c$ might also contribute to

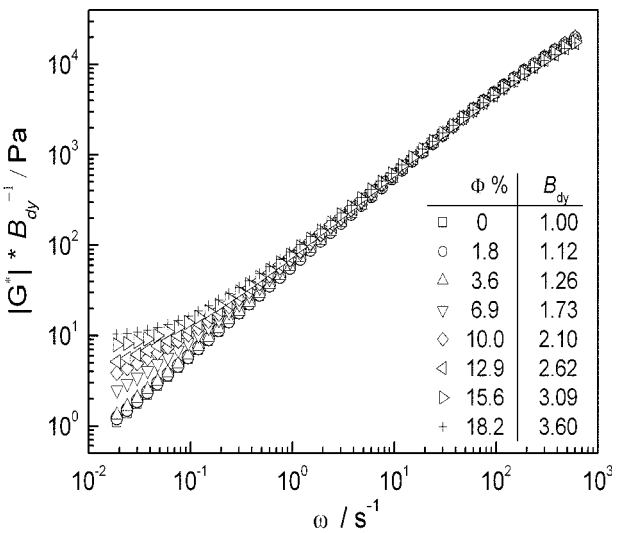

Figure 5 Superposition curve of complex modulus ($|G^*|$) versus frequency (ω) for PDMS/$CaCO_3$ suspensions with different filler volume fraction (Φ).

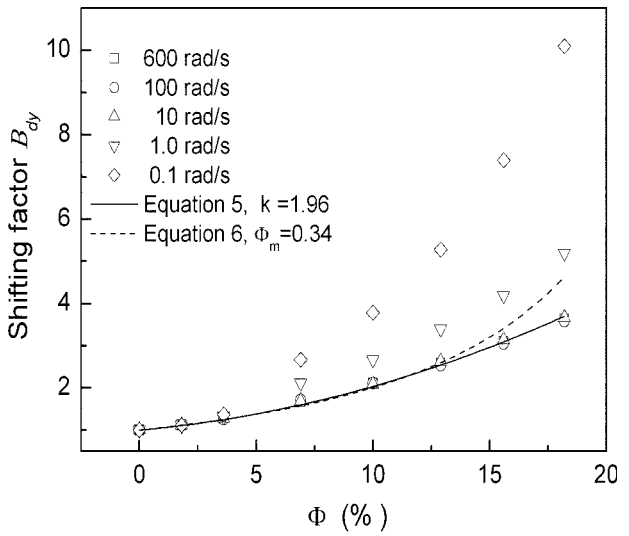

Figure 6 B_{dy} as a function of filler volume fraction (Φ) at different frequencies. The solid and dashed lines are fitted by using eqs. (5) and (6), respectively.

these discrepancies, which will be discussed further in the following section.

Figure 6 gives the plots of B_{dy} as a function of Φ at five different ωs. It is noted that B_{dy} increases with an increase of Φ and the B_{dy} obtained in high ω regions almost coincide with each other within the same Φ; however, deviations appear as ω decreases to 1 rad/s. This phenomenon can also contribute to the discrepancies of the superposition curve in low ω regions as shown in Figure 5. In the field of particle filled polymer systems, the reinforcement effect by filler is usually described by the following relation[20]

$$f(\Phi) = 1 + 2.5\,(k\Phi) + 14.1\,(k\Phi)^2 \tag{5}$$

in which k is an adjustable parameter involving an effective volume fraction of filler particles (particles surrounded by ''bound rubber''). The similarity of the effect of particles on viscosity and modulus (at small deformations or deformation rates) has been justified theoretically.[21] Moreover, the equations describing the flow behavior of an incompressible viscous fluid or of an incompressible elastic material filled with spherical particles conclude a same mathematical form. The solid line in Figure 6 is drawn from fitting the B_{dy} data by eq. (5) with k = 1.96. Meanwhile, we have also plotted the B_{dy} values as dash line on the same graph by using the Krieger-type relation as given by eq. (6), which has been widely employed in the framework of suspension rheology[22]

$$f(\Phi) = \left(1 - \frac{\Phi}{\Phi_m}\right)^{-2} \tag{6}$$

in which Φ_m is a volume fraction corresponding to a maximal volume fraction of filler particles. It can be found that eq. (5) fits the B_{dy} data well as compared with eq. (6), especially in the high Φ regions.

Figure 7 shows the $\dot{\gamma}$ dependence of τ for PDMS/$CaCO_3$ suspensions with different Φ measured at 25°C. Similar to the evolution trend in Figure 2, τ increases with an increase of Φ over the whole $\dot{\gamma}$ regions. However, unlike in dynamic experiments, as compared to the virgin PDMS curve in high $\dot{\gamma}$ regions (>1 s^{-1}), all curves of suspensions shift parallel along abscissa towards smaller $\dot{\gamma}$ direction with increasing Φ. Analogously, in accordance with the ''shear stress equivalent shear rate'' concept,[23,24] this flow behavior can also be described by using a solely concentration-dependent parameter, B_{st}, where the subscript st stands for steady state conditions. Figure 8 depicts the schematic plot of determination for B_{st} through polymer matrix and suspension with Φ = 10%. If these two samples are sheared at a same rate of $\dot{\gamma}_{Susp}$, the corresponding shear stress (τ_1) obtained in the suspension would be larger than that in the polymer matrix τ_0. Hence, to produce shear stress equal to τ_1 in the polymer matrix, one must apply a higher shear rate, $\dot{\gamma}_P > \dot{\gamma}_{Susp}$. The $\dot{\gamma}_P$ can be defined as the ''shear stress equivalent'' shear rate which means that at $\dot{\gamma}_P$ the shear stress produced in the polymer matrix is equivalent to that produced in the suspension at $\dot{\gamma}_{Susp}$. The ratio of these two shear rates, $\dot{\gamma}_P/\dot{\gamma}_{Susp}$, is designated as B_{st}

$$B_{st} = \dot{\gamma}_P(\tau_1)/\dot{\gamma}_{Susp}(\tau_1) \tag{7}$$

It is believed that the deformation history of individual fluid volume elements in concentrated suspen-

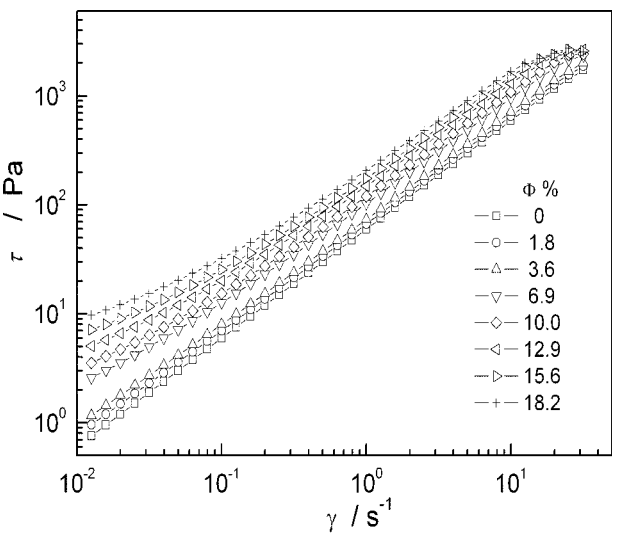

Figure 7 Shear rate ($\dot{\gamma}$) dependence of shear stress (τ) at 25°C for PDMS/$CaCO_3$ suspensions with different filler volume fraction (Φ).

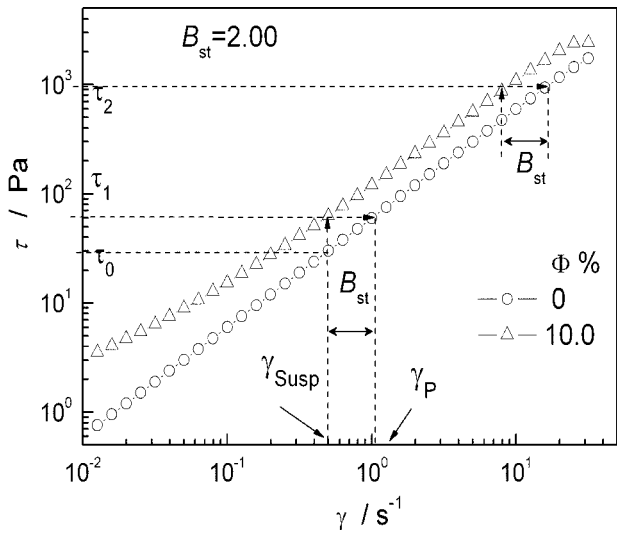

Figure 8 Experimental graphic determination of shifting factor (B_{st}).

sions is extremely complex, even for well-defined monodisperse suspensions filled with spherical particles. The problem is especially complicated when the flow behaviors of suspending liquid are dependent on shear rate, just like the PDMS used here. From a more fundamental view in terms of energy, B_{st} can be understood as an energy dissipation factor. As can be seen in Figure 8, B_{st} is independent of shear stress in the high $\dot{\gamma}$ regions and depends only on the Φ as given by

$$B_{st} = \frac{\dot{\gamma}_P(\tau_1)}{\dot{\gamma}_{Susp}(\tau_1)} = \frac{\dot{\gamma}_P(\tau_2)}{\dot{\gamma}_{Susp}(\tau_2)} = f(\Phi) \quad (8)$$

It is found that this experimental finding makes it possible to collapse the shear stress curve of suspensions onto that of polymer matrix through multiplying $\dot{\gamma}_{Susp}$ by B_{st}. Figure 9 shows the superposition curve of τ versus $\dot{\gamma}$ for the suspensions with different Φ. Similar trend to Figure 5 can be observed; the curves of suspension with $\Phi < \Phi_c$ almost coincide with the virgin PDMS curve over the whole $\dot{\gamma}$ regions. However, the superposition only holds in high $\dot{\gamma}$ regions for suspensions with $\Phi > \Phi_c$. This can also be explained as far as the formation of percolated filler network structure and contributions of yielding phenomenon are concerned.

Figure 10 presents a comparison between $\eta(\dot{\gamma})$ and $|\eta^*(\omega)|$ as a function of $\dot{\gamma}$ and ω for PDMS/$CaCO_3$ suspensions with different Φ. It is obvious that the suspension with $\Phi < \Phi_c$ obey the ''Cox-Merz'' rule, excluding the separation of $\eta(\dot{\gamma})$ curve upon high $\dot{\gamma}$ because of sample structure fracture. However, this rule breakdowns for suspensions with $\Phi > \Phi_c$. The reason for this phenomenon can be attributed to the contributions of hydrodynamic forces which strongly depend on ω and the flow behavior of polymer matrix. For suspensions with low Φ, the hydrodynamic forces of system are predominant over particle–particle interactions because of the viscous nature of polymer matrix. As Φ increases up to Φ_c the particle–particle interactions play a dominant role, leading to the deviations of data collected from different experimental modes. Moreover, the formation of percolated filler network structure also contributes to the divergence. On the other hand, a Newtonian region in viscosity of suspension with $\Phi < \Phi_c$ can be observed for both the $\eta(\dot{\gamma})$ and $|\eta^*(\omega)|$ curves in the low shear regions; whereas for suspensions with $\Phi > \Phi_c$, no Newtonian region was detected together with an increase of viscosities as ω decreases, indi-

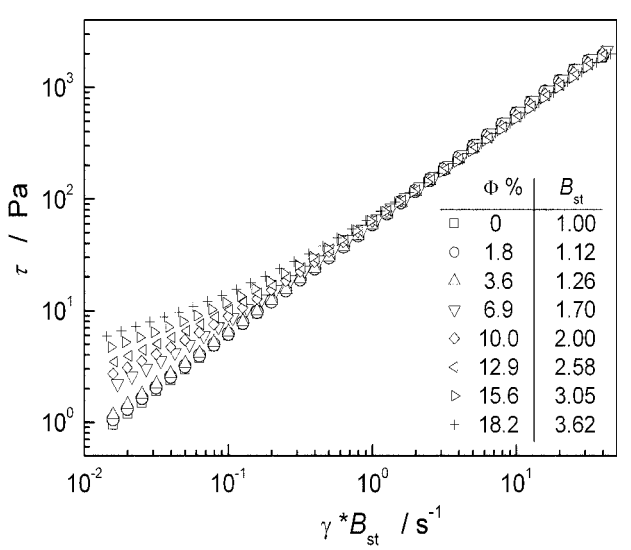

Figure 9 Superposition curve of shear stress (τ) versus shear rate ($\dot{\gamma}$) for PDMS/$CaCO_3$ suspensions with different filler volume fraction (Φ).

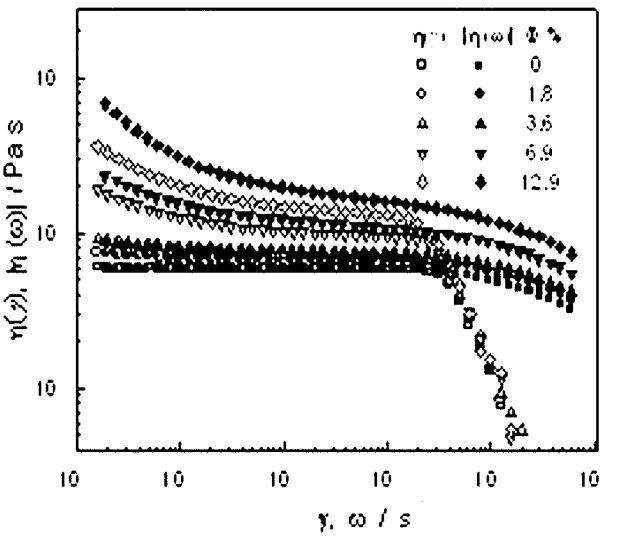

Figure 10 Comparison between the steady state ($\eta(\dot{\gamma})$, open) and complex viscosity ($|\eta^*(\omega)|$, filled) as a function of shear rate ($\dot{\gamma}$) and frequency (ω) for PDMS/$CaCO_3$ suspensions with different filler volume fraction (Φ).

cating an apparent yielding phenomenon. This provides, from another aspect, an evidence of predominance by particle–particle interactions for suspensions with $\Phi > \Phi_c$ as stated previously.

Figure 11 presents the superposition curve of PDMS/$CaCO_3$ suspensions with different Φ, which consists of reduced complex modulus $|G^*(\omega, \Phi)|/B$ as a function of ω, and shear stress $\tau(\dot{\gamma}, \Phi)$ as a function of $B\dot{\gamma}$. This superposition curve is constructed by shifting the $|G^*|$ curves with the shifting factor $B(\Phi)$ along the ordinate, and the τ curves with the shifting factor $B(\Phi)$ along the abscissa. It is seen that a reasonable superposition of all curves is obtained in the high shear regions. One can thus modify the ''Cox-Merz'' rule in a simple fashion for the application of suspensions as given as

$$\frac{|\eta^*(\omega)|}{B(\Phi)} = \frac{\eta(B \cdot \dot{\gamma} = \omega)}{B(\Phi)} = \eta(\dot{\gamma} = \omega)_{\Phi=0} \qquad (9)$$

In this form, the ''Cox-Merz'' relation is valid for both dynamic and steady shear flows in the high shear regions. Figure 12 shows the superposition curve of $\eta(\dot{\gamma})$ and $|\eta^*(\omega)|$ versus $\dot{\gamma}$ and ω for the same samples. Similar to Figure 11, all curves could collapse well in the high shear regions. Unfortunately, only a narrow superposition range is observed due to sample structure fracture upon high $\dot{\gamma}$ in steady shear experiments.

CONCLUSIONS

The steady and dynamic rheological properties of hydroxyl-terminated PDMS filled with $CaCO_3$ particles were investigated based on the ''Cox-Merz'' and modified ''Cox-Merz'' rule. It is found that for the suspensions tested there exists a critical Φ (Φ_c = 3.6%), i.e., percolation threshold, below which both the ''Cox-Merz'' and modified ''Cox-Merz'' rule are competent over the whole shear regions. The reason for this can be ascribed to the predominance of hydrodynamic forces of polymer matrix over particle–particle interactions. However, these two rules breakdown for suspensions with $\Phi > \Phi_c$ which are attributed to the exhibition of an apparent yielding phenomenon and the formation of filler network structure due to filler–filler and filler–polymer interactions, and TEM observations confirm this conclusion. On the other hand, using a concentration-dependent parameter, $B(\Phi)$, superposition curves of dynamic complex modulus ($|G^*|$) (or dynamic complex viscosity $|\eta^*(\omega)|$) as a function of ω and shear stress (τ) (or steady viscosity $\eta(\dot{\gamma})$) as a function of $\dot{\gamma}$ for all PDMS/$CaCO_3$ suspensions were obtained by shifting $|G^*|$ curves along the ordinate and τ functions along the abscissa taking $B(\Phi)$ as shifting factor. Because of the changes of sample microstructure with increasing Φ, the reasonable superposition range is restricted in the high shear regions.

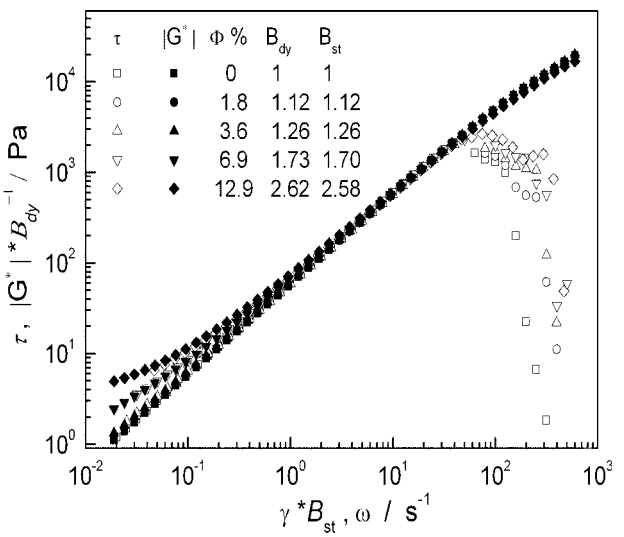

Figure 11 Superposition curve of shear stress (τ, open) and complex modulus ($|G^*|$, filled) for PDMS/$CaCO_3$ suspensions with different filler volume fraction (Φ).

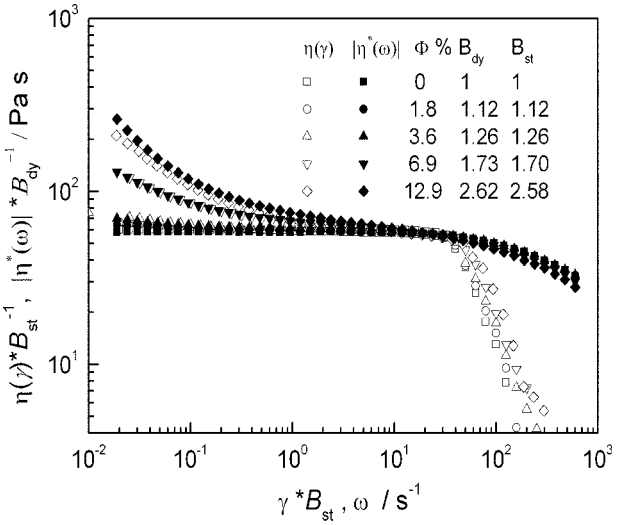

Figure 12 Superposition curve of steady viscosity ($\eta(\dot{\gamma})$, open) and complex viscosity ($|\eta^*(\omega)|$, filled) for PDMS/$CaCO_3$ suspensions with different filler volume fraction (Φ).

References

1. Hanson, D. E.; Hawley, M.; Houlton, R.; Chitanvis, K. Polymer 2005, 46, 10989.
2. Bingham, E. C. Fluidity and Plasticity; McGraw-Hill: New York, 1992.
3. Mill, C. C. Rheology of Disperse Systems, Pergamon: New York, 1959.
4. Gong, G. B.; Xie, H.; Yang, W.; Li, Z. M. Polym Test 2006, 25, 98.
5. Saad, A. L. G.; Younan, A. F. Polym Degrad Stab 1995, 50, 133.

6. Wang, Y. L.; Wu, Q.; Fu, Q. Chem J Chin Univ 2002, 23, 2011.
7. Ferry, J. D. Viscoelastic Properties of Polymers, 3rd ed.; Wiley: New York, 1980.
8. Nielsen, L. E.; Landel, R. F. 2nd ed. Marcel Dekker: New York, 1994.
9. Xu, X. M.; Song, Y. H.; Zheng, Q.; Hu, G. H. J Appl Polym Sci 2006, 103, 2027.
10. Xu, X. M.; Tao, X. L.; Zheng, Q.; Chin J Polym Sci, to appear.
11. Cox, W. P.; Merz, E. H. J Polym Sci 1958, 28, 619.
12. Silva, D.; Oliverira, J. C.; Rao, M. A. Int J Food Properties 1998, 1, 23.
13. Wen, Y. H.; Lin, H. C.; Li, C. H.; Hua, C. C. Polymer 2004, 45, 8551.
14. Berg, R. F. J Rheol 2004, 48, 1365.
15. Lynch, R.; Meng, Y.; Filisko, F. E. J Colloid Interface Sci 2006, 297, 322.
16. Manero, O.; Bautista, F.; Soltero, J. F. A. J.; Puig, E. J Non-Newtonian Fluid Mech 2002, 106, 1.
17. DeGroot, J. V. C.; Macosko, W. J Colloid Interface Sci 1999, 217, 86.
18. Wu, G.; Song, Y. H.; Zheng, Q.; Du, M.; Zhang, P. J. J Appl Ploym Sci 2003, 88, 2160.
19. Walberer, J. A.; Mchugh, A. J. J Rheol 2001, 45, 187.
20. Guth, E.; Gold, O. Phys Rev 1938, 533, 22.
21. Leblanc, J. L. Prog Polym Sci 2002, 27, 627.
22. Krieger, I. M.; Dougherty, T. J Trans Soc Rheol 1959, 3, 137.
23. Gleissle, W.; Baloch, M. K. Proceedings of the 8th International Conference on Slurry Transport, San Francisco, 1983; p 103.
24. Gleissle, W.; Baloch, M. K. Advances in Rheology; Acapulco, 1984; p 549.